https://doi.org/10.5194/wcd-2022-27
Preprint. Discussion started: 3 May 2022

Weather and Climate Dynamics Discussions
Open Access
EGU

Supercell Convective Environments in Spain based on ERA5: Hail and Non-Hail Differences

Carlos Calvo-Sancho[1], Javier Díaz-Fernández[2], Yago Martín[3], Pedro Bolgiani[2], Mariano Sastre[2], Juan Jesús González-Alemán[4], Daniel Santos-Muñoz[5], José Ignacio Farrán[1] and María Luisa Martín[1,6],

[1]Department of Applied Mathematics, Faculty of Computer Engineering, University of Valladolid, Segovia, Spain.
[2]Department of Earth Physics and Astrophysics, Faculty of Physics, Complutense University of Madrid, Madrid, Spain.
[3]Department of Geography, Faculty of History and Philosophy, University Pablo de Olavide, Sevilla, Spain.
[4]State Meteorological Agency (AEMET), Madrid, Spain.
[5]Danmarks Meteorologiske Institut, Copenhaguen, Denmark.
[6]Institute of Interdisciplinary Mathematics (IMI), Complutense University of Madrid, Madrid, Spain.

Correspondence to: Carlos Calvo-Sancho (carlos.calvo.sancho@uva.es)

Abstract. Severe convective storms, in particular supercells, are occasionally responsible for a large number of losses of property and damages in Spain. This paper aims to study the synoptic configurations and pre-convective environments in a dataset of 262 supercells during 2011-2020 in Spain. The events are grouped into supercells with hail (diameter larger than 5 cm) and without hail and the results are compared. ERA5 reanalysis data are used to study the synoptic configurations and soundings related to the supercell events at the initial and centroid time. Moreover, temperature, convective available potential energy, convective inhibition, lifting condensation level, level of free convection, height of freezing level, wind shear and storm-relative helicity are determined for each event. The results show that supercells are more frequent in the Mediterranean coast during the warm season. There are statistically significant differences between hail and non-hail events in the mentioned thermodynamic and kinematic-related parameters analyzed, such as supercells with hail environments characterized by higher median values of most-unstable convective available potential energy than supercells without hail.

1 Introduction

Convective storms and their associated phenomena (lightning, hail, wind or flash-floods) have a great influence on human activities due to the destructive consequences they may have (Martín et al., 2020; Taszarek et al., 2020a; Rodriguez and Bech, 2021). Europe is regularly threatened by severe convective storms (Dahl, 2006), causing considerable economic loss, social impact, and endangering aviation safety (Nisi et al., 2016; Mohr et al., 2017; Antonescu et al., 2017; Kunz et al., 2020; Chernokulsky et al., 2020 Gatzen; et al., 2020). Thus, improving the knowledge on the genesis and life of convective storms is a constant endeavor in the meteorological community.

Thunderstorm cells can be formed either in a discrete and isolated form, or in large and organized systems, e.g., squall-lines. Based on their structure, organization, and size, three different thunderstorm types are defined by the US National Weather Service (NWS, 2019): ordinaries, multicell and supercells. Concerning supercells, Browning (1962) defines them as a

https://doi.org/10.5194/wcd-2022-27
Preprint. Discussion started: 3 May 2022

convectives storm, occurring in a significantly vertically-sheared environment, that contains a deep and persistent mesocyclone, representing the most organized, severe and long-lasting form of isolated deep convection phenomena. These systems are linked with hail reports -including hail diameters larger than 5 cm- and EF2 tornadoes or higher (Duda and Gallus, 2010; Quirantes et al., 2014). Supercells are common phenomena in spring and summertime (Brooks et al., 2019), and can be easily detected through ground-based or satellite lightning detection systems (Bedka et al., 2018; Galanaki et al., 2018). However, the local phenomena associated with these systems, such as hail, require observational reports to be confirmed. As many of these events occur in unpopulated areas, the observed weather reports have a spatial bias toward the most populated areas (Groenemeijer et al., 2017; Edwards et al., 2018). In recent years, thunderstorm reports have increased due to the accessibility of the general population to new technologies, especially thanks to smart-phones and social networks. This has allowed an improvement in databases related to convective storms, with increasing availability of the information on these phenomena (Elmore et al., 2014; Krennert et al., 2018; Taszarek et al., 2020b). Nevertheless, a rigorous quality and validity control, through observational data (radar, satellite…), should be applied to these observational reports to be scientifically valid, e.g., European Severe Weather Database (Dotzek et al., 2009).

Due to orography and land-sea interactions, supercells in Europe tend to be smaller, both horizontally and vertically, than those formed in the US, and therefore show reduced rotation and shorter life spans (Quirantes et al., 2014; Taszarek et al., 2020b). In the particular case of Spain, the study of severe convective storms has grown, extending the knowledge about these systems in recent years. Martin et al. (2020) found more than a hundred supercells per year on average in Spain. Weather environments conducive to severe convective storms have been identified in different studies suggesting that synoptic environments (Merino et al., 2013; Mora et al., 2015), mesoscale characteristics (García-Ortega et al., 2012), orography (Romero et al., 1998) and convective parameters (Calvo-Sancho and Martin, 2021) should be considered together in the research of supercells. Castro et al. (1992) explored the role of topography in the formation and evolution of convective storms in the Ebro Valley (Figure 1a), concluding that mountainous terrain affects the supercells' trajectories and velocities. Studies related to severe weather phenomena, such as hail, lightning, or tornadoes, have been also relevant. Salvador et al. (2021) looked into the charge structure favoring cloud-to-ground lightning in a severe convective storm, concluding that a very high upper-positive charge region is related with a strong updraft and higher cloud-ground rates. Regarding hailstorms, Merino et al. (2019) highlight that the main triggers of convection are thermal instability and low-level convergence. López and Sánchez (2009) reveal the large occurrence of these events in northeastern Spain, causing substantial damages for the local economy, especially in crop fields. Nevertheless, tornadoes occurrence and intensity are not as severe as in other regions of the world due to the absence of wet fluxes inland (Rodríguez and Bech, 2018). Gayà (2011) performed a climatology of tornadoes and waterspouts in Spain and Rodríguez and Bech (2018, 2020) surveyed the mesoscale environments wherein tornadoes and waterspouts formed in the Iberian Peninsula. Both studies reveal that wind shear (WS) plays a more important role than Convective Available Potential Energy (CAPE) in synoptic and mesoscale environments in the cold season.

Since severe supercells have caused substantial property damage and economic losses in recent years in Spain, with around 300 casualties due to severe convective storms from 1987 to 2020 (Consorcio de Compensación de Seguros, 2020), this study

https://doi.org/10.5194/wcd-2022-27
Preprint. Discussion started: 3 May 2022

aims to provide a better understanding of the supercell synoptic and mesoscale environments. To do this, a set of events are selected from the supercell database of Martin et al. (2020) which are then categorized into two distinct groups, i.e., with hail diameter larger than 5 cm (SP-HAIL) and without hail (SP-NONHAIL). These systems are analyzed through their synoptic and mesoscale environments using ERA5 reanalysis (Hersbach et al., 2020). ERA5 is a state of the art, high-resolution reanalysis, which has shown successful results in studies related to severe local storm environments over North America (Coffer et al., 2020; Li et al., 2020; Taszarek et al., 2020a, 2020b), severe convective storms across Europe (Taszarek et al., 2020a, 2020b; Calvo-Sancho and Martín 2021), tornadic environments in the Iberian Peninsula (Rodríguez and Bech, 2020) and microbursts (Bolgiani et al., 2020).

This work is organized as follows. The database and methodology are described in Section 2. Section 3 shows the discussion of the main results related to synoptic and mesoscale environments associated with SP-HAIL and SP-NONHAIL events. Finally, the main conclusions are summarized in Section 4.

2 Data and methodology

2.1 Datasets

The supercell sample used is selected from the Spanish Supercell Database (Martín et al., 2020) for the 2011-2020 period. This dataset is formed by confirmed and medium-high confidence (detected in radar images but without direct observation; see Figure 4 in Martín et al. 2020) supercell events through reports from volunteers and collaborators. Thanks to volunteers, 20.5% of the medium-high confidence supercells were confirmed by two-dimensional radar images. In total, this dataset is formed by 1758 supercells, from which 262 of them correspond to confirmed supercells and 1495 to medium-high confidence supercells. It's worth noting that even if the database covers all the Spanish territories, there are no events reported in the Canary Islands. The database defines the supercell spatial life cycle through an ellipse in a Geographical Information System (Figure 1b). Furthermore, the Spanish Supercell Database collects additional information associated with the events, e.g., hail diameter, tornado intensity. In the current study, only the confirmed supercells are selected and grouped according to the presence of hail with diameters greater than 5 cm (SP-HAIL and SP-NONHAIL). It should be noted that, despite the name given, SP-NONHAIL supercells may contain small hail (less than 5 cm). The initial formation time (t_0) and the ellipse centroid time (t_c) of each supercell are selected to evaluate differences in two different life phases of the systems. The t_0 is selected to characterize the development phase of the cell, while the t_c corresponds to the maturity state. The centroid location is characterized by the geometric center of the ellipse, being t_c the closest time to the middle point of the supercell lifespan (Figure 1b).

The ERA5 reanalysis (Hersbach et al., 2020) is selected to study the synoptic characteristics and the convective variables involved in the supercell development. This is the 5th generation reanalysis created by the European Centre for Medium-Range Weather Forecasts (ECMWF) It is provided with a horizontal grid resolution of 0.25º x 0.25º, 1 hour as temporal resolution and 37 pressure levels for the vertical resolution, from 1000 hPa to 1 hPa. In the current work, the domain is delimited to

https://doi.org/10.5194/wcd-2022-27
Preprint. Discussion started: 3 May 2022

60ºN/20ºN x 30ºW/30ºE to study the environments related to the supercells in Spain. To analyze the mesoscale setting, a vertical profile of temperature, dew point, geopotential height, pressure, and wind components (u, v) are derived from the ERA5 grid for each supercell event.

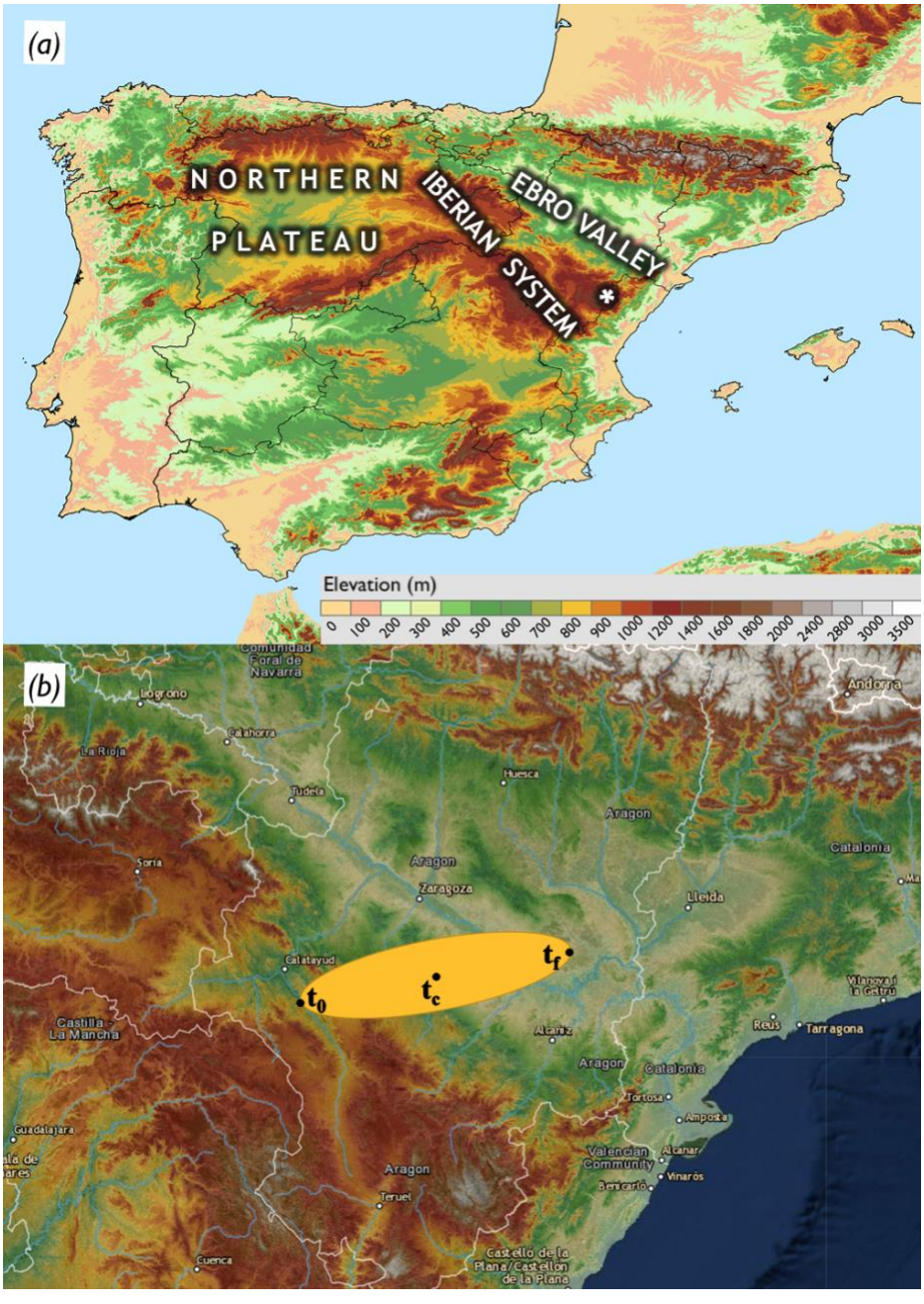

Figure 1: (a) Domain and orography of the study area (m). White star is referred to Maestrazgo area. (b) Example of a supercell ellipse track from Spanish Supercell Database. Basemap source: Spanish Supercell Database Visor (arcg.is/1bPe9n).

https://doi.org/10.5194/wcd-2022-27
Preprint. Discussion started: 3 May 2022

Weather and Climate Dynamics Discussions
Open Access
EGU

2.2 Compositing methodology

Following the methodology of Calvo-Sancho and Martin (2021) and Gensini et al. (2021), supercell soundings for SP-HAIL and SP-NONHAIL events are built for t_0 and t_c. Each vertical profile is computed from ERA5 using the average of the nearest 9 grid points to the supercell location, covering an area of 0.75º x 0.75º (Figure S1, Supplementary). Thus, we avoid the variability that would result from choosing a single grid point and cover an area adequate enough to be representative of the mesoscale conditions. A quality control is carried out to remove any sounding related to convective boundary propagation (Brooks et al. 2003, 2007; Gensini et al. 2021). Accordingly, each vertical profile must record a non-zero Most-Unstable Convective Available Potential Energy (MUCAPE) to be included in the study. Once the vertical profiles are obtained, composites for SP-HAIL and SP-NONHAIL are derived at t_0 and t_c.

Synoptic patterns composites of both events are created to describe and compare the common large-scale features at t_0 and t_c. The ERA5 atmospheric fields used to compute the composites are: 500 and 300 hPa geopotential height, mean sea level pressure, dew point, wind direction and wind speed at 10 meter above sea level, 700-400 hPa integrated mean of omega vertical velocity, and 0-6 km WS. These atmospheric variables have been used in studies related to spatial patterns of hailstorms (Merino et al., 2013; Melcón et al., 2017), supercells (Gropp and Davenport, 2018) and thunderstorms (Mora et al., 2015).

2.3 Convective environments methodology

To characterize the convective environments, the previous 0.75º x 0.75º grid at t_c is used (Figure S1, Supplementary). Several thermodynamic and kinematic variables are calculated for each vertical profile. The selection of these parameters (Table 1) is based on similar studies related to severe convective storms in US and Europe (Rasmunssen et al., 1998; Kaltenböck et al., 2009; Westermayer et al., 2017; Rodríguez and Bech, 2018, 2020; Taszarek et al., 2020; Davenport, 2021). The 2-meter temperature (T2M) and dew-point (DWPT) are computed. CAPE and Convective Inhibition (CIN) using most-unstable (MU), mixed-layer (ML) and surface-based (SB) parcels are calculated using the virtual temperature correction (Doswell and Rasmussen, 1994). The deep-layer bulk wind shear over 0-6 km (WS06) and the effective bulk wind difference [EBWD; limited to the layer in which CAPE ≥ 100 J kg^{-1} and CIN ≥ -250 J kg^{-1}; Thompson et al., 2007] are calculated. . Finally, other parameters relevant to SP-HAIL are also included: ML lifting condensation level (MLLCL), ML level of free convection (MLLFC), height of freezing level (FZH) and height of wet-bulb freezing level (FZH_W).

https://doi.org/10.5194/wcd-2022-27
Preprint. Discussion started: 3 May 2022

Table 1. Parameters used in the mesoscale settings

Parameter	Abbreviation	Units
Thermodynamic parameters		
2-meter temperature	T2M	ºC
2-meter dew-point temperature	DWPT	ºC
Parcel parameters		
Most-unstable convective available potential energy	MUCAPE	J Kg^{-1}
Surface-based convective available potential energy	SBCAPE	J Kg^{-1}
Mixed-layer convective available potential energy	MLCAPE	J Kg^{-1}
Most-unstable convective inhibition	MUCIN	J Kg^{-1}
Surface-based convective inhibition	SBCIN	J Kg^{-1}
Mixed-layer convective inhibition	MLCIN	J Kg^{-1}
Mixed-layer lifting condensation level	MLLCL	m
Mixed-layer level of free convection	MLLFC	m
Height of freezing level	FZH	m
Height of wet-bulb freezing level	FZH_W	m
Kinematic parameters		
Deep-layer bulk wind shear over 0-6 km	WS06	m s^{-1}
Effective bulk wind difference	EBWD	m s^{-1}
Storm-relative helicity over 0-1 km	SRH01	m^2 s^{-2}
Storm-relative helicity over 0-3 km	SRH03	m^2 s^{-2}

The application of the non-parametric Mann-Witney test (Mann and Whitney, 1947) is used to establish statistical differences (at $p < 0.05$) between the SP-HAIL and SP-NONHAIL groups for the above-mentioned parameters. Based on this Mann-Whitney Test, an initial analysis between the t_c and t_0 differences is carried out (Table 2). The results show that there are almost no differences between t_0 and t_c for the same group of supercells (only MLCIN for SP-NONHAIL is significant). Thus, evaluating each group at two different times will not yield any additional information from analyzing only one time step. When the type of cells is compared at the same time, most of the variables result statistically different, and only MUCIN and WS06 show a different statistical significance between t_0 and t_c. As a consequence, for the sake of simplicity, we chose to evaluate only t_c for those results where the assessment of both times would be redundant. This is based on the fact that SP-HAIL and SP-NONHAIL are statistically different for WS06 at t_c, but not at t_0. This variable is much more interesting than MUCIN, as there are other buoyancy terms which can be evaluated while WS06 is a major factor for severe convective environments (Weisman and Klepm, 1982; Brooks et al., 2003; Taszarek et al., 2017).

https://doi.org/10.5194/wcd-2022-27
Preprint. Discussion started: 3 May 2022

Table 2. p-values of the Mann-Whitney test for all the variables analyzed for SP-HAIL and SP-NONHAIL events at t_0 and t_c. p-values equal or lower than 0.05 are in bold.

	SP-HAIL t_c SP-HAIL t_0	SP-NONHAIL t_c SP-NONHAIL t_0	SP-HAIL t_c SP-NONHAIL t_c	SP-HAIL t_0 SP-NONHAIL t_0
MUCAPE	0.95	0.31	**0.00**	**0.00**
SBCAPE	0.81	0.54	**0.00**	**0.00**
MLCAPE	0.84	0.45	**0.00**	**0.00**
T2M	0.67	0.14	**0.00**	**0.00**
DWPT	0.80	0.13	**0.00**	**0.00**
SBCIN	0.85	0.21	**0.00**	**0.00**
MLCIN	0.69	**0.04**	**0.02**	**0.00**
MUCIN	0.99	0.16	0.12	**0.04**
MLLCL	0.54	0.06	0.43	0.38
MLLFC	0.25	0.74	**0.03**	**0.00**
FZH	0.59	0.97	**0.00**	**0.00**
FZH_W	0.53	0.71	**0.00**	**0.00**
WS06	0.72	0.81	**0.04**	0.13
EBWD	0.74	0.18	**0.00**	**0.00**
SRH01	0.76	0.68	0.78	0.77
SRH03	0.40	0.29	0.18	0.36

3 Results and discussion

The spatial and temporal distribution of supercells for both SP-HAIL and SP-NONHAIL formed in the Spanish mainland are first assessed. The main results relative to large-scale composites, and the thermodynamic and kinematic variables involved in supercell formation in the domain are presented and discussed in the following two subsections.

The spatial distribution of the reported supercell episodes (Figure 2a) shows that most of the events for both SP-HAIL and SP-NONHAIL took place in the eastern half of Spain. The Ebro Valley and the Mediterranean coastal area accumulate 79.9% of the SP-NONHAIL and 88.3% of SP-HAIL. This is consistent with lightning observations in Spain, as the eastern Iberian System area (white star in Figure 1a) has the highest density of lightning flash per year (Mora et al. 2019). This area favors convective initiation and supercell formation due to low-level convergence (northwesterly-southeasterly and south westerly-easterly winds), upper-level forcing for ascent, low-medium level moist coming from the Mediterranean Sea and strong diurnal heating (Mora et al. 2015).

The temporal distribution of supercell events (Figure 2b) matches with the warmest and stronger insolation months (July and August accumulate 53.3% of the SP-NONHAIL and 74.4% of the SP-HAIL storms) in the study area, since deep convection

https://doi.org/10.5194/wcd-2022-27
Preprint. Discussion started: 3 May 2022

is a necessary condition to the formation of supercells (Markowski and Richardson, 2010; Miglietta et al., 2017; Taszarek et al., 2019). This is consistent with other studies on convective storms in Europe that assess the higher thunderstorm frequency in summertime, when the diurnal heating is stronger (Kotroni and Lagouvardos, 2016; Taszarek et al., 2018; Taszarek et al., 2019). The hourly distribution of the supercells (Figure 2c) shows a concentration of the events during the late afternoon (summer Local Time is UTC+2), shortly after the daily insolation maximum in the study area. However, the results also yield a large persistence of the conditions, as many events are reported well into the evening.

https://doi.org/10.5194/wcd-2022-27
Preprint. Discussion started: 3 May 2022

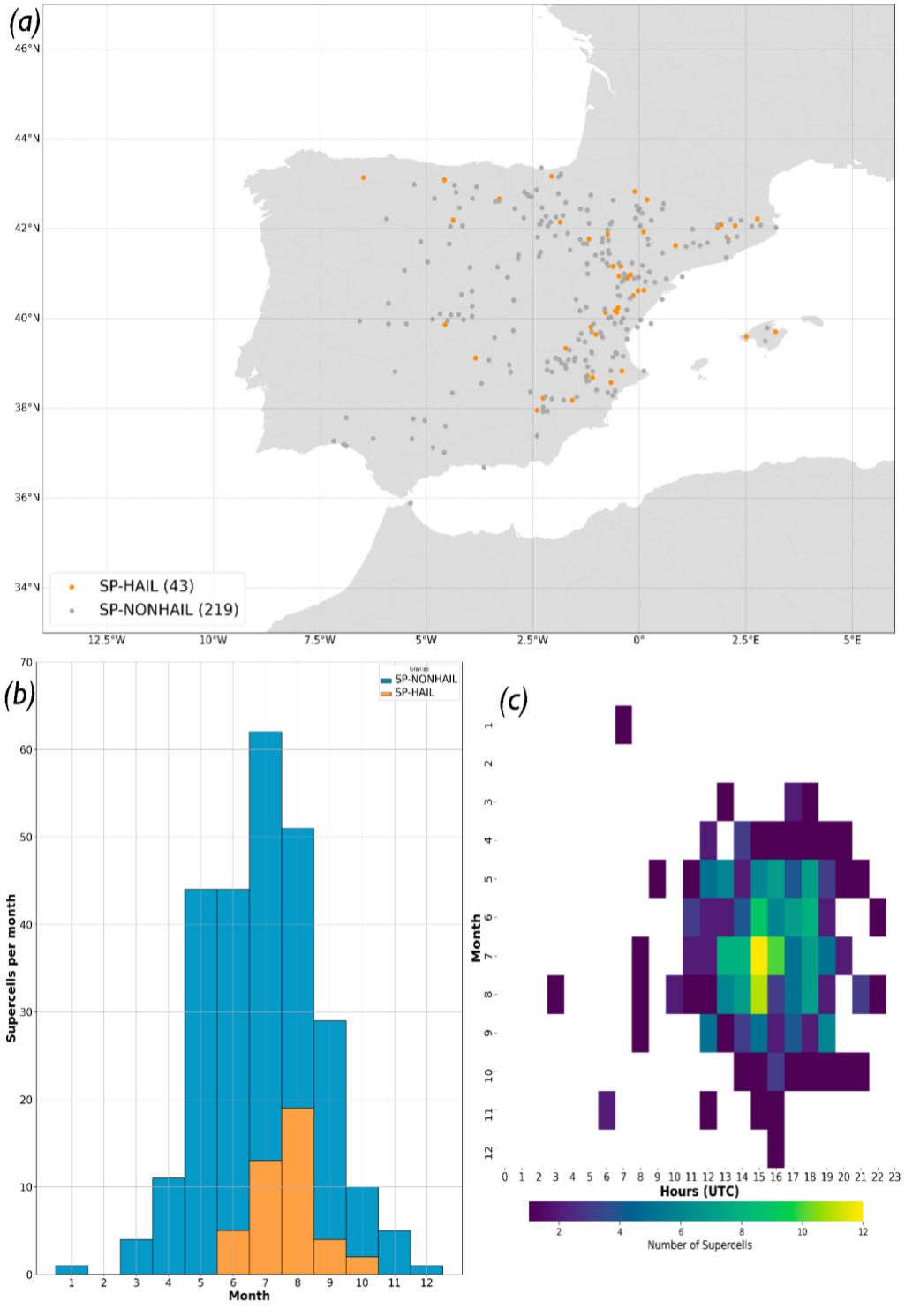

Figure 2: (a) Location of the dataset events (SP-HAIL and SP-NONHAIL) from 2011 to 2020 in Spain. (b) Monthly supercell distribution. (c) Hourly supercell distribution (t_0; UTC).

https://doi.org/10.5194/wcd-2022-27
Preprint. Discussion started: 3 May 2022

3.1 Large-scale setting synoptic features

Synoptic pattern composites for the most relevant atmospheric variables in SP-HAIL and SP-NONHAIL events are shown in this subsection to describe and compare the large-scale characteristics associated with the supercells' formation (t_0) and mature (t_c) phases.

Non-substantial differences between SP-HAIL and SP-NONHAIL are found in the mean sea level pressure (Figure 3). However, the 500 hPa geopotential height displays a SP-NONHAIL composite with a deeper trough and weaker geopotential height gradient, in comparison with SP-HAIL. A similar situation is shown by the 300 hPa geopotential height. This atmospheric configuration promotes weak WS in upper-levels, which could be indicative of weaker convective environments (Weisman and Klemp, 1982; Brooks et al., 2003; Taszarek et al., 2017). Although there are differences between SP-HAIL and SP-NONHAIL, both geopotential configurations promote upper-level positive vorticity advection (not shown) and divergence over Spain, which favor a stronger upper-level forcing (Markowski and Richardson, 2010). Values of 1.1 Pa^{-1} s^{-3} at 700-400 hPa thickness of **Q**-vector divergence are found over eastern Spain. These values indicate forcing for ascent where supercells could have been originated by strong convection (Figure S2, Supplementary). Thermal lows (1012 hPa) can also be appreciated in the center of Spain (Figure 3). These lows are typical of the summer months (Tullot, 2000), promoting east wind flows and ensuring humidity from the Mediterranean Sea in the supercell formation area favoring the initiation of deep convection. Thus, a more favorable environment for deep-moist convection should be expected for SP-HAIL, as the corresponding composite shows a deeper thermal low, covering a larger area and accompanied by an enhanced easterly flow.

Mora et al. (2015) studied electrically severe convective storms in the northern plateau of Spain during 2000-2010, finding that 31% of these thunderstorm episodes were linked to upper-level troughs. These episodes were characterized by strong baroclinic small waves and deep troughs at 500 hPa, which is a pattern very similar to the one shown in SP-HAIL and SP-NONHAIL composites in Figure 3, respectively. Therefore, the results are in line with Mora et al. (2015), showing that supercell episodes in Spain are associated with troughs at upper and medium levels of the troposphere. Overall, it can be seen that the higher convective activity is located on the eastern of Spain, corresponding to the right side of the troughs, with the thermal lows at the center of Spain.

https://doi.org/10.5194/wcd-2022-27
Preprint. Discussion started: 3 May 2022

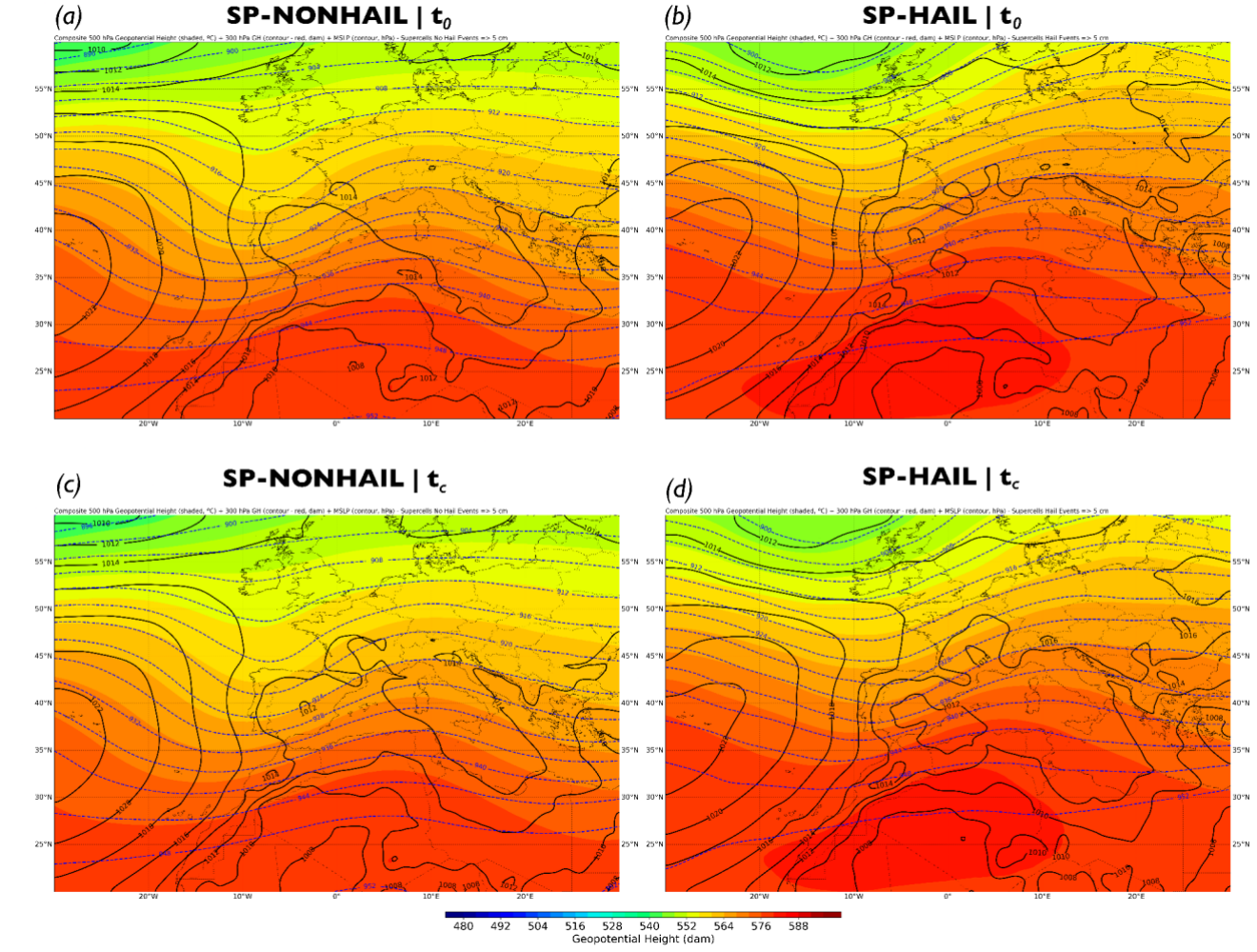

Figure 3: 500 hPa geopotential height (coloured; dam), 300 hPa geopotential height (blue contours; dam) and mean sea level pressure (black lines; hPa) composites for (a) SP-NONHAIL at t_0, (b) SP-HAIL at t_0, (c) SP-NONHAIL at t_c and (d) SP-HAIL at t_c.

One of the main features favoring the deep-moist convection is the moist at lower and medium levels (Taszarek et al., 2019). Figure 4 depicts statistically significant differences in the DWPT values between SP-HAIL and SP-NOHAIL in the Mediterranean Sea and the Atlantic Ocean surrounding Spain, being clearly higher for the first case. Over the land, a notable difference in DWPT is seen for SP-HAIL over the Ebro Valley (Figure 4b, d), along with a stronger eastern wind flow. This would be a result from the geopotential and thermal low configuration described above, which induces the advection of humid air from the Mediterranean. The favorable environment created is then assisted by a triggering of convection west of the Ebro Valley. The high elevations of the Iberian System (> 1400 meters), with a particular mention for the Maestrazgo area (white star in Figure 1a), reduce the role of convective inhibition (Momblona, 2017), which is also met by the convergence of southwestern and eastern surface winds. This initiates the deep convection process that will later develop in the Ebro Valley,

https://doi.org/10.5194/wcd-2022-27
Preprint. Discussion started: 3 May 2022

pushed by the south-westerly flow. This process is consistent with the results of the supercell observations for the period 2011-2020 (Figure 2a).

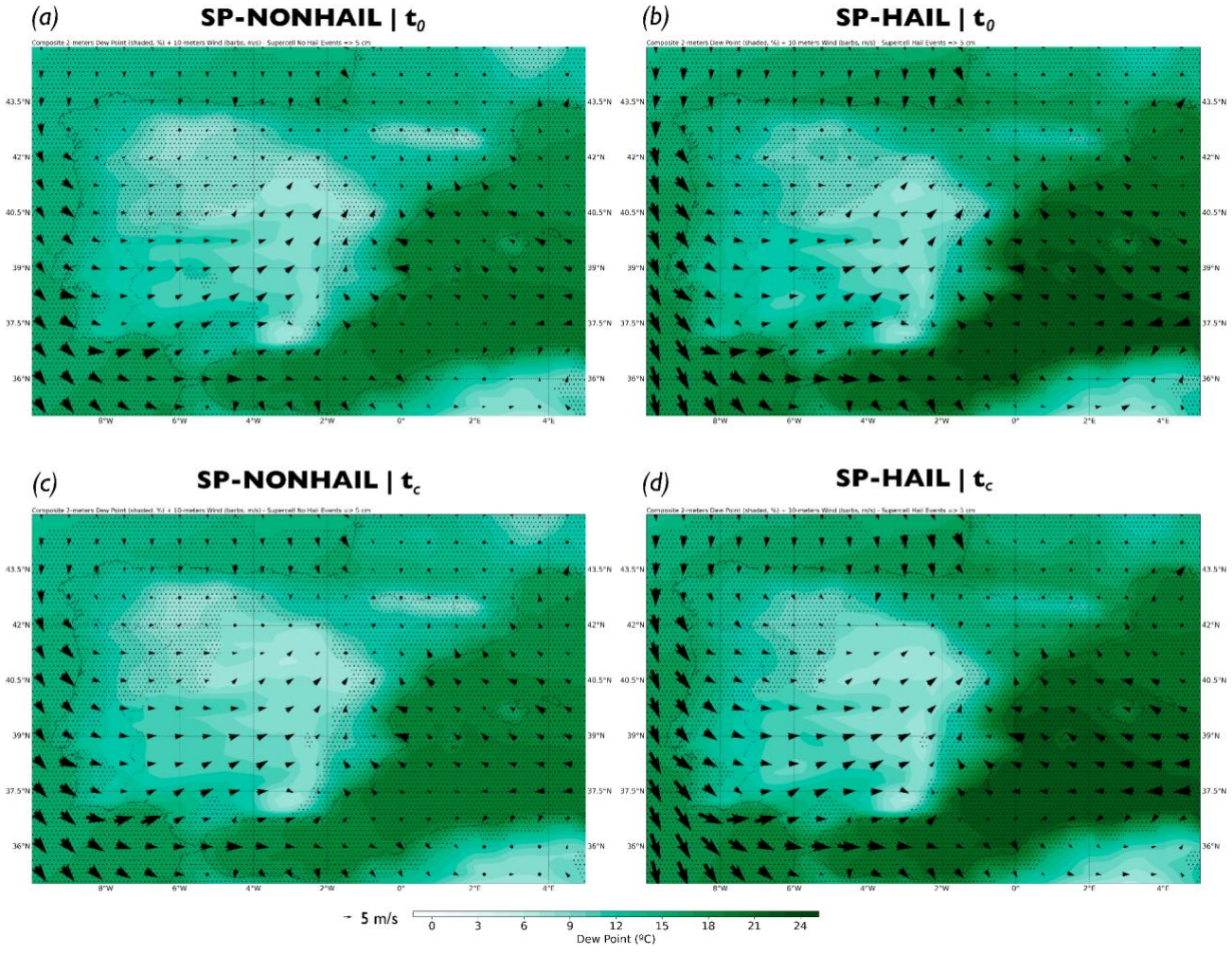

Figure 4: 2-m dew point temperature (contours; ºC) and 10 meters wind (arrows; m s^{-1}) composites for (a) SP-NONHAIL at t_0, (b) SP-HAIL at t_0, (c) SP-NONHAIL at t_c and (d) SP-HAIL at t_c. Black points denote statistically significant differences (p-value < 0.05) in dew point temperature.

The omega vertical velocity composites show statistically significant differences between SP-HAIL and SP-NONHAIL at t_c (Figure 5). The omega maxima for both supercell groups throughout the life cycle of the systems are located in the Ebro valley axis and the Iberian System Mountains, where supercells are most common (Figure 2a). This maxima omega area (-0.3Pa s^{-1}) matches with positive **Q**-vector divergence values (1.1 Pa^{-1} s^{-3}) and convergence of **Q**-vectors (Figure S2, Supplementary) in SP-HAIL events. The maxima omega vertical velocity at 700-400 hPa thickness in SP-HAIL is larger than SP-NONHAIL at t_c with higher values of maxima omega in SP-NONHAIL at 850-500 hPa (not shown). These higher SP-HAIL omega vertical velocity along with the low-level wind convergence (Figure 4b) favor the convection initiation (Markowski and Richardson,

https://doi.org/10.5194/wcd-2022-27
Preprint. Discussion started: 3 May 2022

2010). Sustained omega vertical velocities (Figure 5d) and winds convergence (Figure 4d) enhance and reinforce deep-moist convection at t_c, favoring large hail formation over the Ebro Valley and the Mediterranean area (Gutierrez and Kumjian, 2021). Vertical WS promotes storm organization and its longevity. However, excessive WS can be unfavorable to weak updrafts in environments of low instability and, furthermore, can be disadvantageous to convection initiation by increasing entrainment (Markowski and Richardson, 2010). Figure 5 shows similar values of WS06, for both SP-HAIL and SP-NONHAIL, being moderate (10-20 m s^{-1}) to strong (> 20 m s^{-1}). The conjunction of upper-level forcing (Figure 3), low-level convergence (Figure 4) and strong omega vertical velocity (Figure 5) promotes organization, longevity and severity in the convective storm systems.

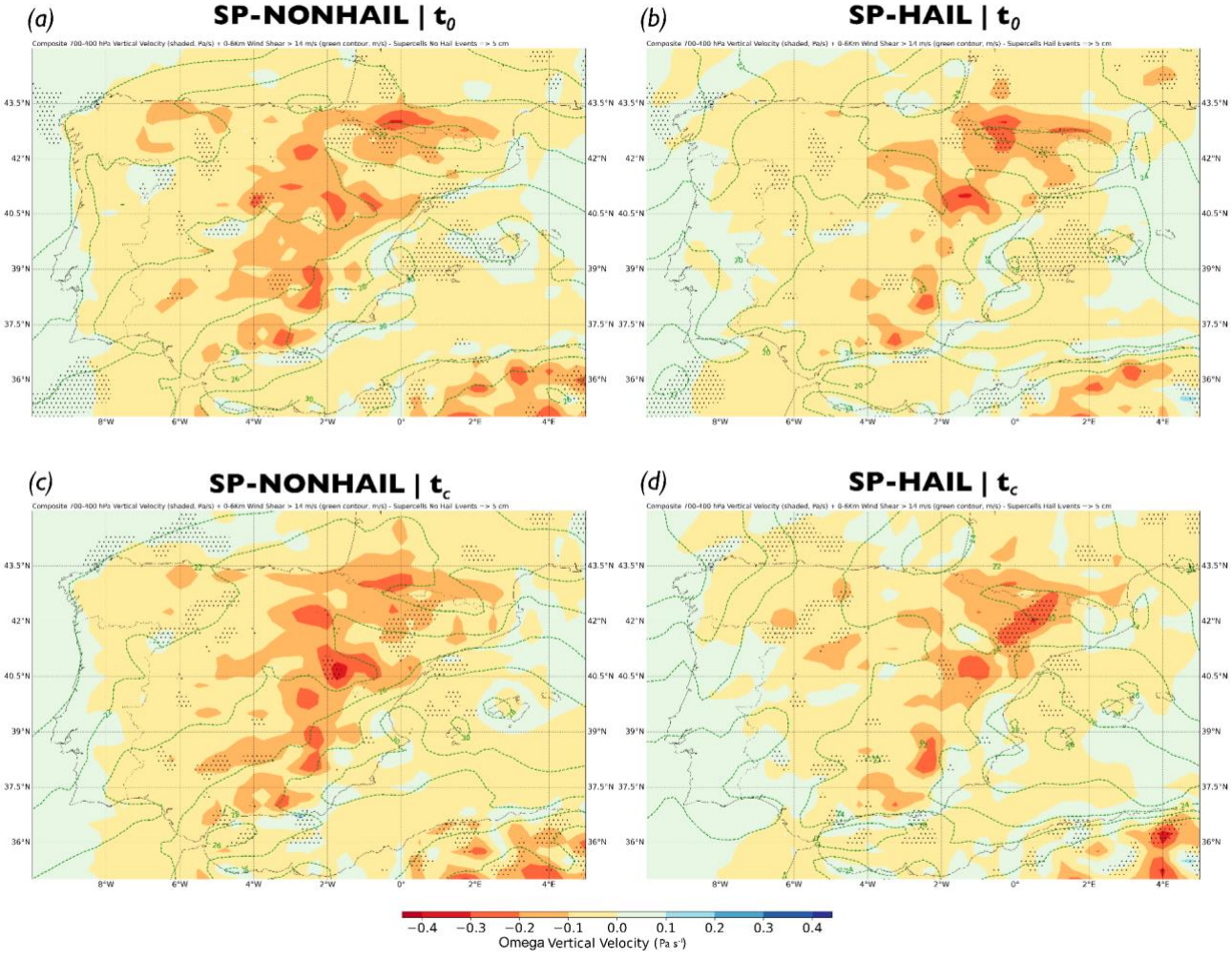

Figure 5: 700-400 hPa omega vertical velocity (contours; Pa s^{-1}), 0-6 km WS (green lines; m s^{-1}) composites for (a) SP-NONHAIL at t_0, (b) SP-HAIL at t_0, (c) SP-NONHAIL at t_c and (d) SP-HAIL at t_c. Black points denote statistically significant differences (p-value < 0.05) in omega vertical velocity.

https://doi.org/10.5194/wcd-2022-27
Preprint. Discussion started: 3 May 2022

3.2 Mesoscale settings

As described in the convective environments methodology (Section 2.3), results of the T2M, DWPT, CAPE, CIN, MLLCL, MLLFC, FZH and WS variables from the ERA5 database are presented in this subsection. These results are shown as violin plots, where the probability density distributions of each variable can be seen, as well as the differences between SP-HAIL and SP-NONHAIL events at t_c.

Based on the synoptic compositing methodology, schematic SP-HAIL and SP-NONHAIL composite soundings at t_c and t_0 are determined (Figure 6). In order to show the vertical profile of the largest and severe supercells, the 90th percentile (based on MUCAPE values) of the Spanish Supercell Database is selected. The 90th percentile vertical profile for each supercell classification reveals interesting features, particularly on the surface, low-levels, and the convective energy. The composite sounding for SP-HAIL (Figure 6b, d) displays a larger CAPE area and a better buoyancy distribution than for SP-NONHAIL (Figure 6a, c). This high value of CAPE (1877.1 J kg^{-1}) is strongly associated with vertical accelerations (Markowski and Richardson, 2010), so hail formation would be favored. CAPE values are larger at t_0 than at t_c, for both categories. The CIN in SP-HAIL increases from t_0 to t_c, i.e., the stability is increasing through the supercell life cycle which could favor sustained systems and reinforce the vertical motions (Gropp and Davenport, 2018). In contrast, the SP-NONHAIL CIN values do not substantially change (-137.5 J kg^{-1}; Figure 6 a, c). LCL (Figure 6, black dot in panels) and LFC do not show significant changes between SP-HAIL and SP-NONHAIL events. However, the LCL in SP-HAIL exhibits a higher value at t_c in comparison with the value at t_0. According to Mulholland et al. (2021), a higher LCL is related to the width of the deep convective updraft, resulting in a wider, deeper, and faster vertical velocity, which would be in line with the omega vertical velocity results (Figure 5b, d). Wind barbs reveal a moderate WS06 for both types of supercells. This helps to organize convection as the negative effect of precipitation and outflow on the updraft is reduced with large WS values above the updraft height (Markowski and Richardson, 2010). In addition, SP-HAIL low-level WS is higher than SP-NONHAIL, favoring hail growth (Gutierrez and Kumjian, 2021). Also, the sounding composites show large wind values in upper-levels (< 400 hPa), which may favor wind divergence at the upper troposphere and deep-moist convection. The evolution from t_0 to t_c depicts a reduction in WS for SP-HAIL, which is mainly denoted in the wind speed and not in the rotation, contrary to the SP-NONHAIL episodes.

https://doi.org/10.5194/wcd-2022-27
Preprint. Discussion started: 3 May 2022

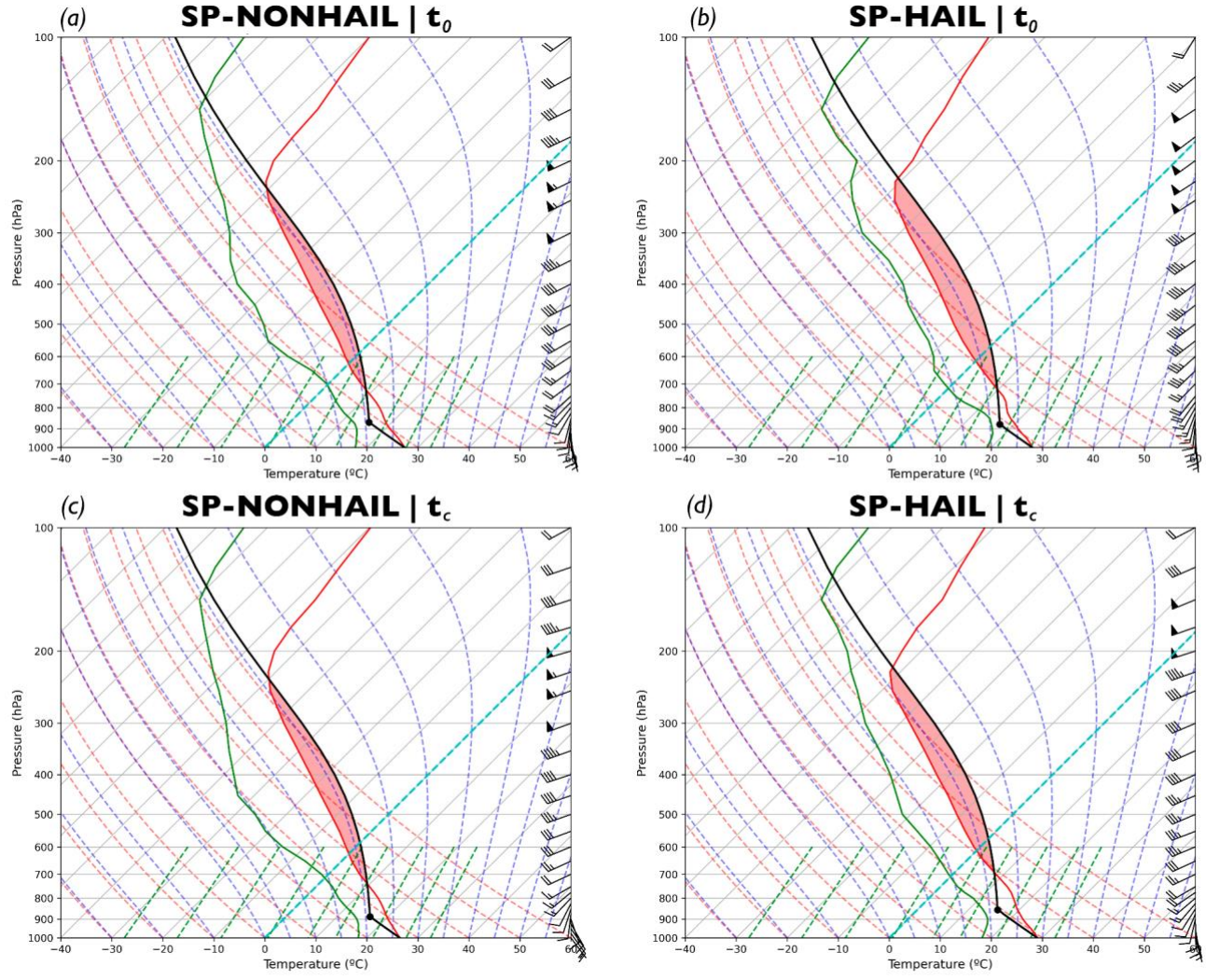

Figure 6: 90th percentile soundings composites for (a) SP-NONHAIL at t_0, (b) SP-HAIL at t_0, (c) SP-NONHAIL at t_c and (d) SP-HAIL at t_c. Black dot indicates the LCL value.

The distribution for T2M and DWPT show differences between both types of events, statistically significant (Table 2) for both variables. Different distributions can be seen in Figure 7. The T2M for SP-HAIL depicts a bimodal distribution with model values of 26 ºC and 31 ºC, approximately, with less variability than the corresponding SP-NONHAIL figure. Moreover, the T2M distribution shows a larger median value for SP-HAIL (Table 3), exhibiting a larger variability for SP-NONHAIL. The T2M maximum (minimum) for SP-HAIL is 35.6 ºC (19.3 ºC), showing a very similar value for SP-NONHAIL while the minimum is significantly lower (11.9 ºC) in SP-NONHAIL. The DWPT amplitudes are similar with greater median values for SP-HAIL than for SP-NONHAIL (Table 3). However, the 25th percentile for SP-NONHAIL (8.5 ºC) is significantly lower than SP-HAIL (12.0 ºC). These differences are mainly originated in the low-level wind flows. In the Spanish Mediterranean area, Balearic Islands and places favorable for maritime fluxes, the main contributor to low-level moisture is advection from

https://doi.org/10.5194/wcd-2022-27
Preprint. Discussion started: 3 May 2022

the warm Mediterranean Sea. However, in the Spanish inland the main contributor would be the evapotranspiration of the crop fields and vegetation (Vicente-Serrano et al. 2014; Tomas-Burguera et al. 2021), contributing considerably less humidity to the environment.

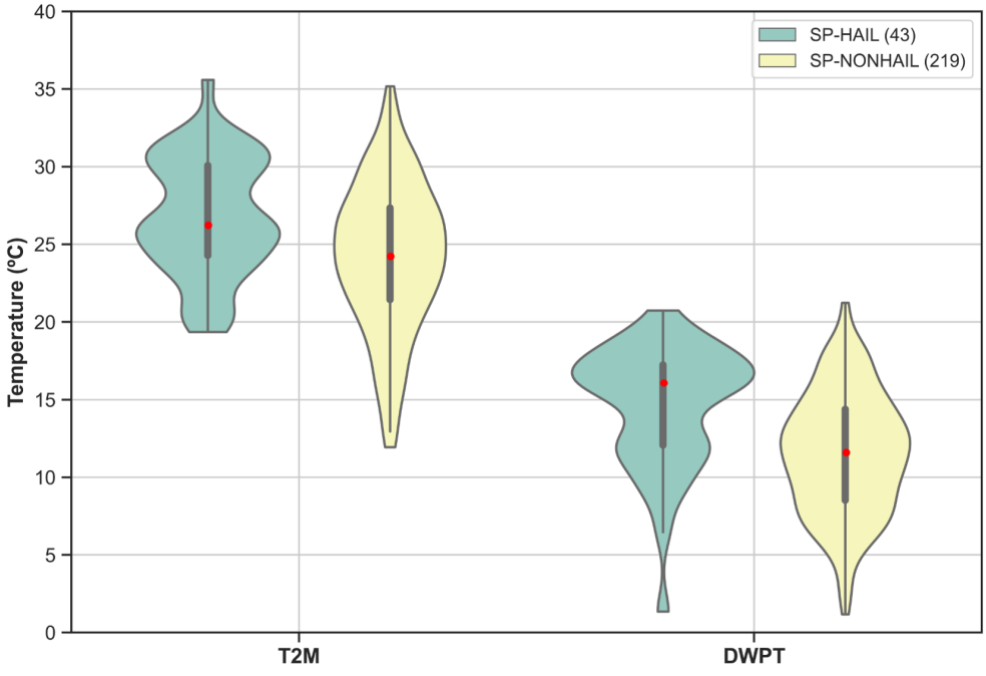

Figure 7: T2M and DWPT distributions and boxplots for SP-HAIL and SP-NONHAIL at t_c. The median is represented as a red point.

Since CAPE is a common and useful forecast tool for predicting supercells and hail (Kaltenböck et al., 2009; Merino et al., 2013), its distributions in the parcel measurements of MUCAPE, SBCAPE and MLCAPE are shown (Figure 8a). The results show statistically significant differences in the distributions for SP-HAIL and SP-NONHAIL (Table 2). It is noteworthy that CAPE's distributions follow positive skew distributions in SP-NONHAIL events, being the SP-HAIL median values notably larger than SP-NONHAIL, but with a lower amplitude. However, the 25th percentile and median values for SP-HAIL SBCAPE, 200 and 600 J kg^{-1}, respectively, are lower than those described by Kaltenböck et al. (2009) for Europe, approximately 400 and 1000 J kg^{-1}. Yet, as CAPE is a variable very dependent on humidity and orography, these differences will arise from the high elevations and relatively low humidity over the domain of study. As expected, MUCAPE and MLCAPE yield larger values for both SP-HAIL and SP-NONHAIL. Kahraman et al. (2017) analyzed the convective storm environments for tornado and severe hail days from 1979 to 2013 in Turkey. In their study, severe storm environments are characterized by smaller CAPE in Turkey compared to US, highlighting that severe hail occurrence is associated with large CAPE and vertical wind shear. In the current analysis, the median value for MUCAPE and MLCAPE (Table 3) in SP-HAIL events agree with those obtained in Kahraman et al. (2017) and Púčik et al. (2015) in their study of severe hail-thunderstorms in central Europe. However, the SBCAPE results are lower than those obtained by Kahraman et al. (2017). This discrepancy might be partially

https://doi.org/10.5194/wcd-2022-27
Preprint. Discussion started: 3 May 2022

attributed to the warmer eastern surrounding seas (Mediterranean and Black Sea; Shaltout and Omstedt, 2014). In Taszarek et al. (2020b) study of severe convective storms with hail, MLCAPE values are greater than for the current study, with values around 1000 and 1200 J kg^{-1} for the US and Europe, respectively. As it is discussed above, supercells in Europe tend to be smaller than the ones formed in the US, with lower rotation values and shorter life spans (Quirantes et al., 2014; Taszarek et al., 2020b).

Table 3. Median values for each parameter analyzed for SP-HAIL and SP-NONHAIL events at t_c.

	SP-HAIL t_c	SP-NONHAIL t_c
MUCAPE	1031	374
SBCAPE	618	145
MLCAPE	746	203
T2M	26	24
DWPT	16	12
SBCIN	-138	-77
MLCIN	-96	-54
MUCIN	-16	-16
MLLCL	1661	1783
MLLFC	2809	2254
FZH	4025	3599
FZH_W	3566	3238
WS06	19	17
EBWD	16	10
SRH01	8	10
SRH03	88	74

Related to severe convective storms in Spain, Merino et al. (2013) analyzes several hailstorm days in the Ebro Valley through high resolution simulations with the WRF model, obtaining a threshold CAPE of 500 J kg^{-1} for hail events. According to Rodriguez and Bech (2018), the CAPE values found in our study would correspond with those for tornadic storms in eastern Spain and the Balearic Islands. These authors analyze a dataset of 907 tornado and waterspout events from 1980 to 2018 using atmospheric profiles from the ERA5 reanalysis and finding SBCAPE values higher than 400 J kg^{-1} in tornadic storms (EF1 or stronger).

https://doi.org/10.5194/wcd-2022-27
Preprint. Discussion started: 3 May 2022

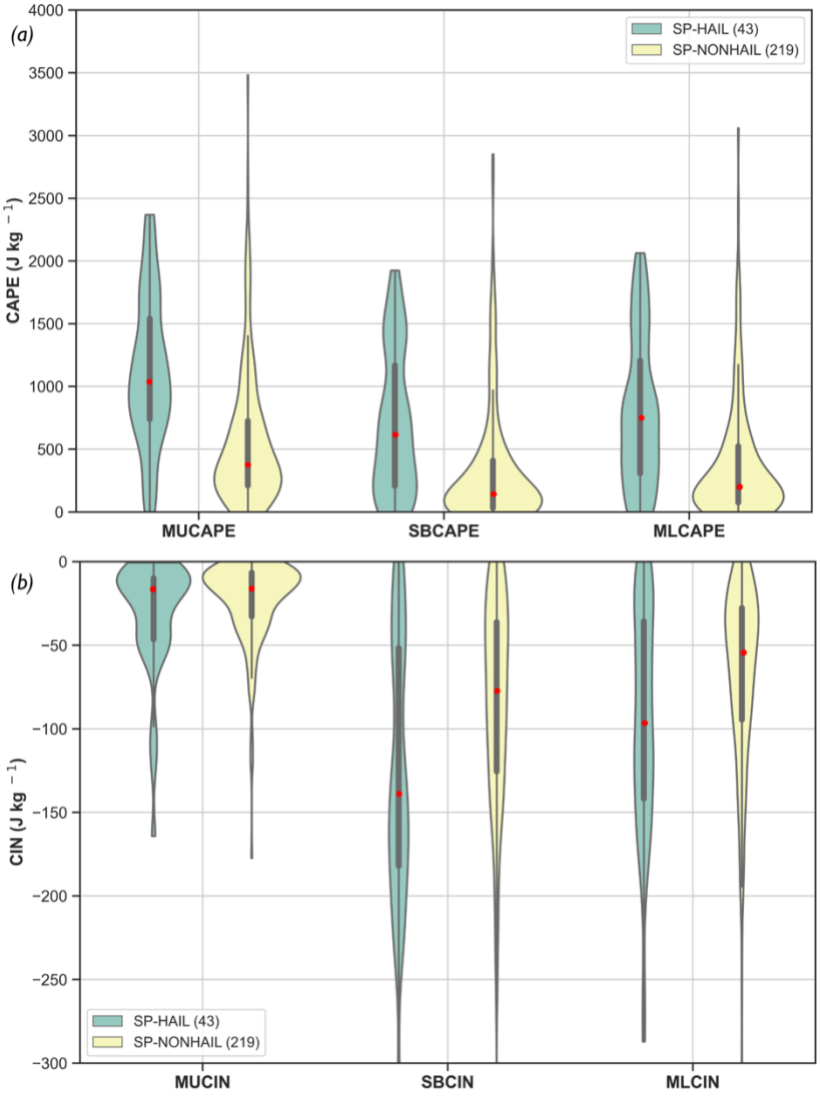

310 **Figure 8: As in Figure 7, but for (a) MUCAPE, SBCAPE and MLCAPE. (b) MUCIN, SBCIN and MLCIN.**

It is well known that ERA5 CIN values do not represent capping inversions in severe weather environments correctly (Nevius and Evans, 2018; Coffer et al., 2020). Here, CIN distribution in the parcel measures MUCIN, SBCIN and MLCIN are displayed (Figure 8b). The SP-HAIL and SP-NONHAIL differences for SBCIN and MLCIN distributions are statistically significant (Table 2). However, MUCIN differences are not statistically significant, presenting negative skew distributions for both events
315 and absolute values lower than for SBCIN and MLCIN. The SP-HAIL events show an important capping inversion layer (Figure 8b), with a MLCIN median of 95.8 J kg^{-1} (Table 3) and of 53.6 J kg^{-1} for SP-NONHAIL. These results contrast with Taszarek et al. (2020b), who concluded MLCIN values for large hail events are lower (~ 50 J kg^{-1}) but similar to those obtained in the US. The higher CIN values obtained in this survey, in comparison with those in Central Europe, could be related with

https://doi.org/10.5194/wcd-2022-27
Preprint. Discussion started: 3 May 2022

the average thermal differences in the summer season (3.5 ºC higher than Central Europe; not shown). The strong insolation and diurnal heating favor this mean temperature difference and, in turn, the thermal low development (Font, 2000). Another cause of the high CIN in Spanish supercells is the complex orography of the Spanish inland. Moreover, enhanced CIN may delay the convective initiation until the CAPE is maximized; once the convection triggers, discrete convective modes, including isolated and elevated supercells, can be developed producing large hail (Rasmussen and Blanchard, 1998; Smith et al., 2012; Thompson et al., 2012, 2013;). Therefore, in light of the SBCIN and MLCIN results, a mechanical trigger to force the mechanism that initiates convection is required and the conjunction of these factors favors great vertical motions and organized convection.

A comparison of MLLCL, MLLFC, FZH and FZH_W percentiles and distributions between SP-HAIL and SP-NONHAIL is performed in Figure 9. The MLLCL has been an important discriminator between tornadic and non-tornadic supercells in the US (Rasmussen and Blanchard, 1998; Thompson et al., 2003). Taszarek et al. (2020b) compare the MLLCL in severe convective storms with hail greater than 5 cm in US and Europe obtaining high similarities between both continents. However, in Europe, the MLLCL tends to have much less variability on supercell events, so the skill of this indicator is limited (Kahraman et al., 2017; Taszarek et al., 2020b). The results here shown for Spain are in line with the previous conclusion, since there are no statistically significant differences (Table 2) for MLLCL between SP-HAIL and SP-NONHAIL events. Rodriguez and Bech (2018) also observe this low MLLCL variability between tornadic and non-tornadic convective storms in the Iberian Peninsula. Nevertheless, Púčik et al. (2015) obtained a MLLCL median value of 1000 m for severe hail-thunderstorms in central Europe, while in the current study the median MLLCL in SP-HAIL events is greater (Table 3). The MLLFC shows significant differences (Table 2) between SP-HAIL and SP-NONHAIL, being higher for SP-HAIL events. It is also remarkable the high variability for both events in comparison with the MLLCL distributions. Comparing the MLLFC values with those obtained by Taszarek et al. (2020) for US and Europe, the domain of study shows a higher altitude and larger variability. The discrepancy between MLLCL and MLLFC altitudes reflects the high MUCIN values observed in Figure 8. Another important factor to SP-HAIL and SP-NONHAIL events is the freezing level, with differences between both types of supercells statistically significant for FZH and FZH_W (Table 2). Both FZH and FZH_W distributions for SP-NONHAIL events present higher variability than for SP-HAIL ones (Figure 9), being the FZH median value for SP-HAIL higher than for SP-NONHAIL (Table 3).

https://doi.org/10.5194/wcd-2022-27
Preprint. Discussion started: 3 May 2022

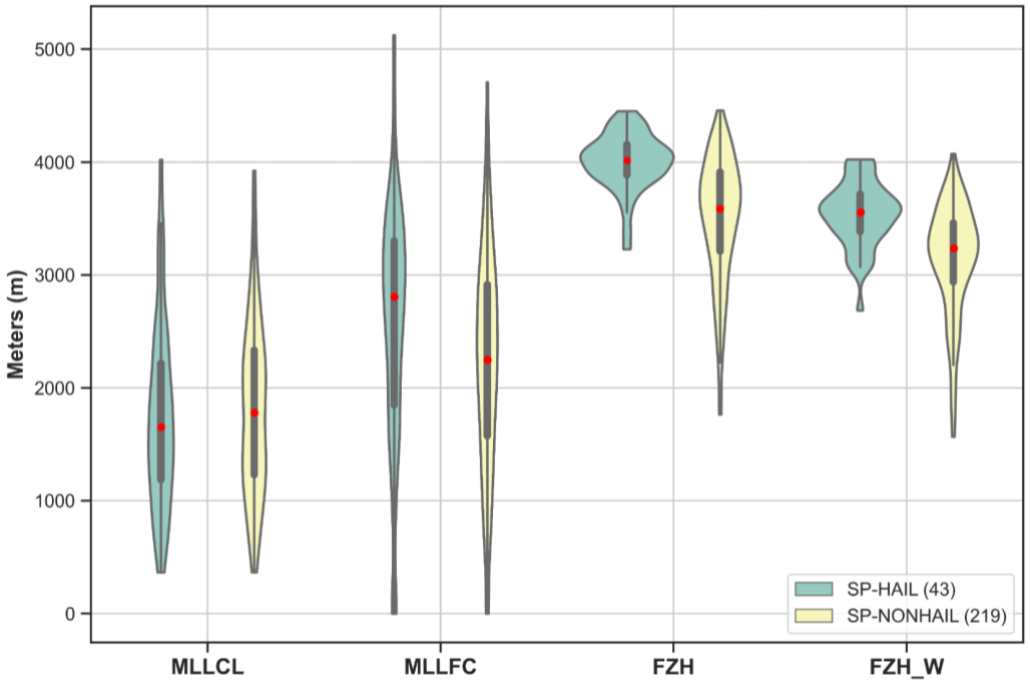

Figure 9: As in Figure 7, but for MLLCL, MLLFC, FZH and FZH_W.

Several studies (Rasmussen and Blanchard, 1998; Púčik et al., 2015; Taszarek et al., 2019) suggest that the severity of the convective storms depend on the relationship between CAPE and WS. Furthermore, deep-moist convection tends to develop more organized systems as the WS intensifies (Markowski and Richardson 2010). WS between 0-6 km and EBWD distributions for SP-HAIL and SP-NONHAIL events are displayed (Figure 10). As expected, the WS06 and EBWD values are higher for SP-HAIL than for SP-NONHAIL with statistically significant differences (Table 2). The WS06 and EBWD median values for SP-HAIL (Table 3) agree with Taszarek et al. (2020b) results for severe convective storms with large hail in Europe; nevertheless, the values for the USA are higher than those presented here. Despite this, SP-HAIL events in the domain of study can be explained by the presence of several mountain ranges in the study area (Figure 1a) where the WS is enhanced by the interaction of the wind field with orography, with a similar mechanism as observed in the Alps (Kunz et al., 2018; Taszarek et al., 2020). However, ERA5 is limited to reproduce this enhancement due to its horizontal resolution.

Helicity is a frequent parameter used for forecasting supercells and tornadoes since it quantifies the cyclonic updraft rotation in right and left moving supercells (in this survey only the right-moving measure is used; Davies-Jones et al., 1990; Bunkers et al., 2002) Environments with high SRH usually enhance the development of the mesocyclones and large hail formation (Rasmussen and Blanchard, 1998; Thompson et al., 2003), revealing SRH as a useful predictor for severe weather with organized convection, such as the supercell cases. The SRH01 and SRH03 distributions show no statistically significant differences (Table 2) between SP-HAIL and SP-NONHAIL. The SRH01 variability for both events is quite similar (Figure S3, Supplementary), being the median value of SP-NONHAIL higher than SP-HAIL. On the other hand, it is remarkable the

https://doi.org/10.5194/wcd-2022-27
Preprint. Discussion started: 3 May 2022

SRH03 high variability for both events in comparison with the SRH01 distribution. The SP-HAIL mature phase has been observed in environments with moderate helicity (Table 2), while SP-NONHAIL has lower SRH03 values. There are remarkable SRH03 maxima for both groups of events with values around 280 $m^2 s^{-2}$ for SP-NONHAIL and 350 $m^2 s^{-2}$ for SP-HAIL, in line with Kahmaran et al. (2017), who state that large hail occurrences are associated with large values of SRH03. Rodriguez and Bech (2018, 2021) obtain similar SRH03 values for EF0 and EF1 tornadoes and waterspouts in Iberia. However, these values are lower than those obtained by Taszarek et al. (2020b) in Europe for large hail reports. The SRH03 results are also consistent with Calvo-Sancho et al. (2021), where the SRH03 median spatial distribution in Spain displays values of almost 100 $m^2 s^{-2}$ in the eastern half of Spain.

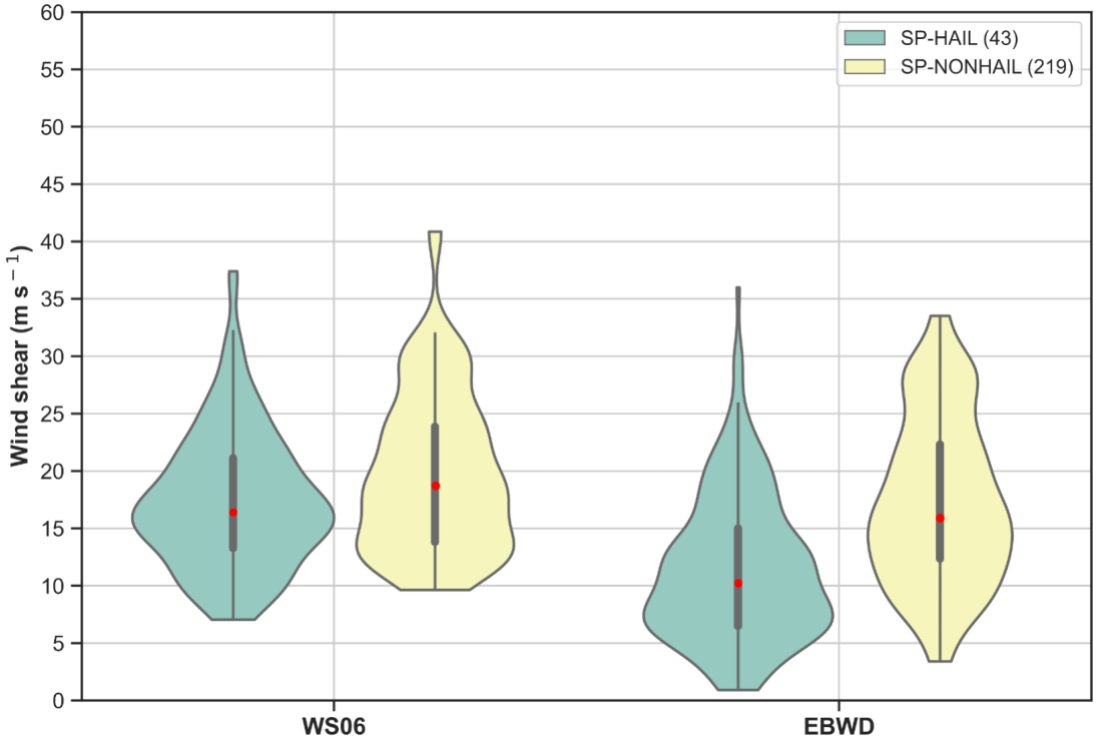

Figure 10: As in Figure 7, but for WS06 and EBWD.

4 Summary and conclusions

The environments of SP-HAIL and SP-NONHAIL events are here characterized and compared in Spain from 2011 to 2020. Different atmospheric variables are retrieved from ERA5 reanalysis to obtain the synoptic patterns and sounding composites at the development time and the mature phase time of the supercells. Thermodynamic and kinematic parameters related to convective environments are also calculated and compared between SP-HAIL and SP-NONHAIL events at the mature phase time for the mesoscale environment analysis.

https://doi.org/10.5194/wcd-2022-27
Preprint. Discussion started: 3 May 2022

The results yield several conclusions; the most important are listed below:

- There are notable differences in the spatial and monthly distributions of supercells between eastern and western Spain. The eastern half of Spain accumulates 79.9% of the SP-NONHAIL and 88.3% of the SP-HAIL events. July and August accumulate 53.3% of the SP-NONHAIL and 74.4% of the SP-HAIL storms.
- The synoptic patterns composites show a deeper trough for SP-NONHAIL in comparison with SP-HAIL composites at 500 hPa with the largest height gradients corresponding to SP-HAIL. Strong upper-level forcing is promoted by vorticity advection and upper-level divergence. Surface humidity is influenced by the 10-meters winds, being higher for SP-HAIL. The conjunction of these factors with wind convergences allows the convection initiation. Omega vertical velocity reveals that the SP-HAIL's updraft is higher, allowing the large hail formation.
- The T2M and DWPT values are related to supercell monthly distributions with higher values corresponding to the warm season and minimum values to the cool season. Both variables are statistically different between SP-HAIL and SP-NONHAIL, being larger for the first group.
- Environments of SP-HAIL events are characterized by approximately three times larger MUCAPE median values than SP-NONHAIL events. Moreover, higher CAPEs, MLLFC, FZH, WS06, EBWD and SRH03 values and lower CIN values are found for SP-HAIL than for SP-NONHAIL. The differences for these parameters between both events are statistically significant at $p < 0.05$, except for SRH03.
- Based on the ERA5 characterization results for SP-HAIL in Spain, 75% of the events present T2M > 24.3 ºC, DWPT > 12.1 ºC, MUCAPE > 740 J kg^{-1}, MLCIN < -36 J kg^{-1}, MLLFC > 1850 m, FZH > 3890 m , FZH_W > 3685 m, WS06 > 14 m s^{-1} and SRH03 > 58 m^2 s^{-2}.

Finally, orography and convective environments have been revealed as important factors to supercell formation and development. Thus, although ERA5 resolution improves previous reanalyses, more research is needed with high-resolution models, allowing the study of the interactions between large-scale and convection processes in the genesis and development of hail supercell events.

Data availability

ERA5 reanalysis is available from the Copernicus Climate Change Service Climate Data Store (https://doi.org/10.24381/cds.bd0915c6, Hersbach et al., 2018). Spanish Supercell Database upon request to the author.

Author contributions

CC-S, JD-F, YM, MLM, PB and JG-A designed the study. CC-S and JD-F performed the analysis and wrote the first manuscript. PB, JG-A, MS, and MLM supervised and review. DSM and JF computational and software support. All authors discussed the results and edited the manuscript.

https://doi.org/10.5194/wcd-2022-27
Preprint. Discussion started: 3 May 2022

Conflicts of Interest

The authors declare that there are no conflicts of interest regarding the publication of this paper.

Acknowledgements.

This work was partially supported by the following research projects: PID2019-105306RB-I00 (IBERCANES project), CGL2016-78702-C2-1-R and CGL2016-78702-C2-2-R (SAFEFLIGHT project), FEI-EU-17-16 and SPESMART AND SPESVALE (ECMWF Special Projects). Carlos Calvo-Sancho and Javier Díaz-Fernández acknowledge the grant supported by the Spanish Ministerio de Ciencia, Innovación y Universidades (FPI programs PRE2020-092343 and BES-2017-080025, respectively). Y. Martin acknowledges the grant supported by the European Union (Marie Skłodowska-Curie Programs 101019424).

References

Antonescu, B., Schultz, D. M., Holzer, A., & Groenemeijer, P. (2017). Tornadoes in Europe: An underestimated threat. Bulletin of the American Meteorological Society, 98(4), 713-728.

Bech, J., Pineda, N., Rigo, T., Aran, M., Amaro, J., Gayà, M., ... & van der Velde, O. (2011). A Mediterranean nocturnal heavy rainfall and tornadic event. Part I: Overview, damage survey and radar analysis. Atmospheric research, 100(4), 621-637.

Bedka, K., Murillo, E. M., Homeyer, C. R., Scarino, B., & Mersiovsky, H. (2018). The above-anvil cirrus plume: An important severe weather indicator in visible and infrared satellite imagery. Weather and Forecasting, 33(5), 1159-1181.

Bolgiani, P., Santos-Muñoz, D., Fernández-González, S., Sastre, M., Valero, F., & Martín, M. L. (2020). Microburst detection with the WRF model: Effective resolution and forecasting indices. Journal of Geophysical Research: Atmospheres, 125(14), e2020JD032883.

Brooks, H. E., Lee, J. W., & Craven, J. P. (2003). The spatial distribution of severe thunderstorm and tornado environments from global reanalysis data. Atmospheric Research, 67, 73-94.

Brooks, H. E., Anderson, A. R., Riemann, K., Ebbers, I., & Flachs, H. (2007). Climatological aspects of convective parameters from the NCAR/NCEP reanalysis. Atmospheric Research, 83(2-4), 294-305.

Brooks, H. E., Doswell III, C. A., Zhang, X., Chernokulsky, A. A., Tochimoto, E., Hanstrum, B., ... & Barrett, B. (2019). A century of progress in severe convective storm research and forecasting. Meteorological Monographs, 59, 18-1.

Calvo-Sancho, C. and Martín, Y. (2021). Supercell Pre-convective Environments in Spain: a dynamic downscaling of ERA-5 Reanalysis, EGU General Assembly 2021, online, 19–30 Apr 2021, EGU21-2967, https://doi.org/10.5194/egusphere-egu21-2967, 2021.

https://doi.org/10.5194/wcd-2022-27
Preprint. Discussion started: 3 May 2022

Calvo-Sancho, C. (2021). Caracterización de los ambientes convectivos que favorecen el desarrollo de la convección organizada en España: exploración y evolución en el período 1979-2019 mediante reanálisis ERA5. Final Master Thesis. Universidad de Zaragoza. http://dx.doi.org/10.13140/RG.2.2.25129.31841

Castro, A., Sánchez, J. L., & Fraile, R. (1992). Statistical comparison of the properties of thunderstorms in different areas around the Ebro-Valley (Spain). Atmospheric research, 28(3-4), 237-257.

Chernokulsky, A., Kurgansky, M., Mokhov, I., Shikhov, A., Azhigov, I., Selezneva, E., ... & Kühne, T. (2020). Tornadoes in northern Eurasia: From the middle age to the information era. Monthly Weather Review, 148(8), 3081-3110.

Coffer, B.E., Taszarek, M., & Parker, M.D. (2020). Near-Ground Wind Profiles of Tornadic and Nontornadic Environments in the United States and Europe from ERA5 Reanalyses. Weather and Forecasting 35, 2621–2638. https://doi.org/10.1175/WAF-D-20-0153.1

Consorcio de Compensación de Seguros. (2020). Estadística de Riesgos Extraordinarios. Serie 1971–220. Accessed January 30, 2022. http://www.consorseguros.es/web/documents/10184/44193/Estadistica_Riesgos_Extraordinarios_1971_2014/14ca6778-2081-4060-a86d-728d9a17c522.

Dahl, J. M. (2006). Supercells: their dynamics and prediction (Doctoral dissertation).

Davis-Jones, R., Burgess, D.W., and Foster, M. (1990): Test of helicity as a forecast parameter. Preprints, 16th Conf. on Severe Local Storms, Kananaskis Park, AB, Canada, Amer. Meteor. Soc., 588–592.

Dotzek, N., Groenemeijer, P., Feuerstein, B., & Holzer, A. M. (2009). Overview of ESSL's severe convective storms research using the European Severe Weather Database ESWD. Atmospheric research, 93(1-3), 575-586.

Duda, J. D., & Gallus, W. A. (2010). Spring and summer midwestern severe weather reports in supercells compared to other morphologies. Weather and forecasting, 25(1), 190-206. DOI: 10.1175/ 2009WAF2222338.1.

Edwards, R., Allen, J. T., & Carbin, G. W. (2018). Reliability and climatological impacts of convective wind estimations. Journal of Applied Meteorology and Climatology, 57(8), 1825-1845.

Elmore, K. L., Flamig, Z. L., Lakshmanan, V., Kaney, B. T., Farmer, V., Reeves, H. D., & Rothfusz, L. P. (2014). mPING: Crowd-sourcing weather reports for research. Bulletin of the American Meteorological Society, 95(9), 1335-1342.

Farnell, C., Rigo, T., & Pineda, N. (2018). Exploring radar and lightning variables associated with the Lightning Jump. Can we predict the size of the hail?. Atmospheric Research, 202, 175-186.

Galanaki, E., Lagouvardos, K., Kotroni, V., Flaounas, E., & Argiriou, A. (2018). Thunderstorm climatology in the Mediterranean using cloud-to-ground lightning observations. Atmospheric Research, 207, 136-144.

García-Ortega, E., Merino, A., López, L., & Sánchez, J. L. (2012). Role of mesoscale factors at the onset of deep convection on hailstorm days and their relation to the synoptic patterns. Atmospheric Research, 114, 91-106.

Gatzen, C. P., Fink, A. H., Schultz, D. M., & Pinto, J. G. (2020). An 18-year climatology of derechos in Germany. Natural Hazards and Earth System Sciences, 20(5), 1335-1351.

https://doi.org/10.5194/wcd-2022-27
Preprint. Discussion started: 3 May 2022

Gayà, M. (2011). Tornadoes and severe storms in Spain. Atmospheric Research 100 (4):334–43. doi: 10.1016/j. Atmosres.2010.10.019.

Gensini, V. A., Converse, C., Ashley, W. S., & Taszarek, M. (2021). Machine Learning Classification of Significant Tornadoes and Hail in the United States Using ERA5 Proximity Soundings. Weather and Forecasting, 36(6), 2143-2160.

Groenemeijer, P., Púčik, T., Holzer, A. M., Antonescu, B., Riemann-Campe, K., Schultz, D. M., ... & Sausen, R. (2017). Severe convective storms in Europe: Ten years of research and education at the European Severe Storms Laboratory. Bulletin of the American Meteorological Society, 98(12), 2641-2651.

Gropp, M. E., & Davenport, C. E. (2018). The impact of the nocturnal transition on the lifetime and evolution of supercell thunderstorms in the Great Plains. Weather and Forecasting, 33(4), 1045-1061.

Gutierrez, R. E., & Kumjian, M. R. (2021). Environmental and Radar Characteristics of Gargantuan Hail–Producing Storms. Monthly Weather Review, 149(8), 2523-2538.

Hamid, K. (2012). Investigation of the passage of a derecho in Belgium. Atmospheric research, 107, 86-105.

Hersbach, H., Bell, B., Berrisford, P., Hirahara, S., Horányi, A., Muñoz-Sabater, J., Nicolas, J., Peubey, C., Radu, R., Schepers, D., Simmons, A., Soci, C., Abdalla, S., Abellan, X., Balsamo, G., Bechtold, P., Biavati, G., Bidlot, J., Bonavita, M., Chiara, G., Dahlgren, P., Dee, D., Diamantakis, M., Dragani, R., Flemming, J., Forbes, R., Fuentes, M., Geer, A., Haimberger, L., Healy, S., Hogan, R.J., Hólm, E., Janisková, M., Keeley, S., Laloyaux, P., Lopez, P., Lupu, C., Radnoti, G., Rosnay, P., Rozum, I., Vamborg, F., Villaume, S., Thépaut, J. (2020). The ERA5 global reanalysis. Q.J.R. Meteorol. Soc. 146, 1999–2049. https://doi.org/10.1002/qj.3803.

Kahraman, A., Kadioglu, M., & Markowski, P. M. (2017). Severe convective storm environments in Turkey. Monthly Weather Review, 145(12), 4711-4725.

Kaltenböck, R., Diendorfer, G., Dotzek, N. (2009). Evaluation of thunderstorm indices from ECMWF analyses, lightning data and severe storm reports. Atmos. Res. 93 (1–3), 381–396.

Kotroni, V., & Lagouvardos, K. (2016). Lightning in the Mediterranean and its relation with sea-surface temperature. Environmental Research Letters, 11(3). https://doi.org/10.1088/1748-9326/11/3/034006

Krennert, T., Pistotnik, G., Kaltenberger, R., & Csekits, C. (2018). Crowdsourcing of weather observations at national meteorological and hydrological services in Europe. Advances in Science and Research, 15, 71-76.

Kuchera, E. L., & Parker, M. D. (2006). Severe convective wind environments. Weather and forecasting, 21(4), 595-612.

Kunz, M., Blahak, U., Handwerker, J., Schmidberger, M., Punge, H. J., Mohr, S., ... & Bedka, K. M. (2018). The severe hailstorm in southwest Germany on 28 July 2013: Characteristics, impacts and meteorological conditions. Quarterly Journal of the Royal Meteorological Society, 144(710), 231-250.

Kunz, M., Wandel, J., Fluck, E., Baumstark, S., Mohr, S., & Schemm, S. (2020). Ambient conditions prevailing during hail events in central Europe. Natural Hazards and Earth System Sciences, 20(6), 1867-1887.

Li, F., Chavas, D. R., Reed, K. A., & Dawson II, D. T. (2020). Climatology of severe local storm environments and synoptic-scale features over North America in ERA5 reanalysis and CAM6 simulation. Journal of Climate, 33(19), 8339-8365.

https://doi.org/10.5194/wcd-2022-27
Preprint. Discussion started: 3 May 2022

Lombardo, K. A., & Colle, B. A. (2011). Convective storm structures and ambient conditions associated with severe weather over the northeast United States. Weather and forecasting, 26(6), 940-956.

López, L., & Sánchez, J. L. (2009). Discriminant methods for radar detection of hail. Atmospheric Research, 93(1-3), 358-368.

Mann, H. B., & Whitney, D. R. (1947). On a test of whether one of two random variables is stochastically larger than the other. The annals of mathematical statistics, 50-60.

Markowski, P., & Richardson, Y. (2011). Mesoscale meteorology in midlatitudes (Vol. 2). John Wiley & Sons.

Martín, Y., Cívica, M., & Pham, E. (2020). Constructing a Supercell Database in Spain Using Publicly Available Two-Dimensional Radar Images and Citizen Science. Annals of the American Association of Geographers, 0(0), 1–21. https://doi.org/10.1080/24694452.2020.1812371.

Melcón, P., Merino, A., Sánchez, J. L., López, L., & García-Ortega, E. (2017). Spatial patterns of thermodynamic conditions of hailstorms in southwestern France. Atmospheric Research, 189, 111-126.

Merino, A., García-Ortega, E., López, L., Sánchez, J. L., & Guerrero-Higueras, A. M. (2013). Synoptic environment, mesoscale configurations and forecast parameters for hailstorms in Southwestern Europe. Atmospheric Research, 122, 183-198.

Miglietta, M.M., Mazon, J. & Rotunno, R. (2017) Numerical simulations of a tornadic supercell over the Mediterranean. Weather and Forecasting, 32, 1209–1226. https://doi.org/10.1175/WAF- D-16-0223.1.

Mohr, S., Kunz, M., & Geyer, B. (2015). Hail potential in Europe based on a regional climate model hindcast. Geophysical Research Letters, 42(24), 10-904.

Mohr, S., Kunz, M., Richter, A., & Ruck, B. (2017). Statistical characteristics of convective wind gusts in Germany. Natural Hazards and Earth System Sciences, 17(6), 957-969.

Momblona, D. (2017). Convección en la Sierra de Gúdar: caso de estudio del 20 de agosto de 2016. AEMET.

Mora, M., Riesco, J., de Pablo Dávila, F., & Rivas Soriano, L. (2015). Atmospheric background associated with severe lightning thunderstorms in Central Spain. International Journal of Climatology, 35(4), 558-569.

Mulholland, J. P., Peters, J. M., & Morrison, H. (2021). How does LCL height influence deep convective updraft width?. Geophysical Research Letters, 48(13), e2021GL093316.

National Weather Service (NWS). (2019). Supercell struc- ture and dynamics. Accessed 21 January 2021. https://www.weather.gov/lmk/supercell/dynamics.

Nevius, D. S., & Evans, C. (2018). The influence of vertical advection discretization in the WRF-ARW Model on capping inversion representation in warm-season, thunderstorm-supporting environments. Weather and Forecasting, 33(6), 1639-1660.

Nisi, L., Martius, O., Hering, A., Kunz, M., & Germann, U. (2016). Spatial and temporal distribution of hailstorms in the Alpine region: a long-term, high resolution, radar-based analysis. Quarterly Journal of the Royal Meteorological Society, 142(697), 1590-1604.

https://doi.org/10.5194/wcd-2022-27
Preprint. Discussion started: 3 May 2022

Púčik, T., Groenemeijer, P., Rýva, D., & Kolář, M. (2015). Proximity soundings of severe and nonsevere thunderstorms in central Europe. Monthly Weather Review, 143(12), 4805-4821.

Quirantes, J. A. (2003). Tornado F2/F3 y Supercélula de Alcañiz (Teruel) [EN: F2/F3 Tornado and Supercell in Alcañiz, Teruel]. Accessed 24 January 2022. http:// www.tiemposevero.es/ver-reportaje.php?id=35.

Quirantes Calvo, J. A., Riesco Martín, J., & Núñez Mora, J. Á. (2014). Características básicas de las supercélulas en España. Agencia Estatal de Meteorología (AEMET).

Rasmussen, E. N., & Blanchard, D. O. (1998). A baseline climatology of sounding-derived supercell and tornado forecast parameters. Weather and forecasting, 13(4), 1148-1164.

Rodríguez, O., & Bech, J. (2018). Sounding-derived parameters associated with tornadic storms in Catalonia. International Journal of Climatology, 38(5), 2400-2414.

Rodríguez, O., & Bech, J. (2021). Tornadic environments in the Iberian Peninsula and the Balearic Islands based on ERA5 reanalysis. International Journal of Climatology, 41, E1959-E1979.

Romero, R., Ramis, C., Alonso, S., Doswell III, C. A., & Stensrud, D. J. (1998). Mesoscale model simulations of three heavy precipitation events in the western Mediterranean region. Monthly weather review, 126(7), 1859-1881.

Shaltout, M., & Omstedt, A. (2014). Recent sea surface temperature trends and future scenarios for the Mediterranean Sea. Oceanologia, 56(3), 411-443.

Smith, B. T., Thompson, R. L., Grams, J. S., Broyles, C., & Brooks, H. E. (2012). Convective modes for significant severe thunderstorms in the contiguous United States. Part I: Storm classification and climatology. Weather and Forecasting, 27(5), 1114-1135.

Taszarek, M., Brooks, H. E., & Czernecki, B. (2017). Sounding-derived parameters associated with convective hazards in Europe. Monthly Weather Review, 145(4), 1511-1528.

Taszarek, M., Brooks, H. E., Czernecki, B., Szuster, P., & Fortuniak, K. (2018). Climatological aspects of convective parameters over Europe: A comparison of ERA-interim and sounding data. Journal of Climate, 31(11), 4281–4308. https://doi.org/10.1175/JCLI-D-17-0596.1

Taszarek, M., Allen, J., Púčik, T., Groenemeijer, P., Czernecki, B., Kolendowicz, L., … Schulz, W. (2019). A climatology of thunderstorms across Europe from a synthesis of multiple data sources. Journal of Climate, 32(6), 1813–1837. https://doi.org/10.1175/JCLI-D-18-0372.1

Taszarek, M., Allen, J. T., Groenemeijer, P., Edwards, R., Brooks, H. E., Chmielewski, V., & Enno, S. E. (2020a). Severe convective storms across Europe and the United States. Part I: Climatology of lightning, large hail, severe wind, and tornadoes. Journal of Climate, 33(23), 10239–10261. https://doi.org/10.1175/JCLI-D-20-0345.1

Taszarek, M., Allen, J.T., Púčik, T., Hoogewind, K.A., & Brooks, H.E. (2020b). Severe Convective Storms across Europe and the United States. Part II: ERA5 Environments Associated with Lightning, Large Hail, Severe Wind, and Tornadoes. Journal of Climate 33, 10263–10286. https://doi.org/10.1175/JCLI-D-20-0346.1.

https://doi.org/10.5194/wcd-2022-27
Preprint. Discussion started: 3 May 2022

Thompson, R. L., Edwards, R., Hart, J. A., Elmore, K. L., & Markowski, P. (2003). Close proximity soundings within supercell environments obtained from the Rapid Update Cycle. Weather and Forecasting, 18(6), 1243-1261.

Thompson, R. L., Smith, B. T., Grams, J. S., Dean, A. R., & Broyles, C. (2012). Convective modes for significant severe thunderstorms in the contiguous United States. Part II: Supercell and QLCS tornado environments. Weather and forecasting, 27(5), 1136-1154.

Thompson, R. L., Smith, B. T., Dean, A. R., & Marsh, P. T. (2013). Spatial distributions of tornadic near-storm environments by convective mode. E-Journal of Severe Storms Meteorology, 8(5).

Tomas-Burguera, M., Beguería, S., & Vicente-Serrano, S. M. (2021). Climatology and trends of reference evapotranspiration in Spain. International Journal of Climatology, 41, E1860-E1874.

Tullot, I. F. (2000). Climatología de España y Portugal (Vol. 76). Universidad de Salamanca.

Vicente-Serrano, S. M., Azorin-Molina, C., Sanchez-Lorenzo, A., Revuelto, J., López-Moreno, J. I., González-Hidalgo, J. C., ... & Espejo, F. (2014). Reference evapotranspiration variability and trends in Spain, 1961–2011. Global and Planetary Change, 121, 26-40.

Weisman, M. L., & Klemp, J. B. (1982). The dependence of numerically simulated convective storms on vertical wind shear and buoyancy. Monthly Weather Review, 110(6), 504-520.

Westermayer, A., Pucik, T., Groenemeijer, P., & Tijssen, L. (2016). Comparison of sounding observations and reanalysis of thunderstorm environments. In Eighth European Conf. on Severe Storms.